Quantified effect of seawater biogeochemistry on the temperature dependence of sea spray aerosol fluxes

Karine Sellegri[1], Theresa Barthelmeß[2], Jonathan Trueblood[1], Antonia Cristi[3], Evelyn Freney[1], Clémence Rose[1], Neill Barr[3], Mike Harvey†, Karl Safi[4], Stacy Deppeler[3], KarenThompson[4], Wayne Dillon[5], Anja Engel[2] and Cliff Law[3,5]

[1]Université Clermont Auvergne, CNRS, Laboratoire de Météorologie Physique (LaMP) F-63000 Clermont-Ferrand, France
[2] GEOMAR, Helmholtz Centre for Ocean Research Kiel, 24105 Kiel, Germany
[3] National Institute of Water and Atmospheric Research (NIWA), Wellington, New Zealand
[4] National Institute of Water and Atmospheric Research (NIWA), Hamilton, New Zealand
[5] Department of Marine Science, University of Otago, Dunedin, New Zealand
†Deceased

Correspondence to: Karine Sellegri (karine.sellegri@uca.fr)

Abstract. Future change in sea surface temperature may influence climate via various air-sea feedbacks and pathways. In this study, we investigate the influence of surface seawater biogeochemical composition on the temperature dependence of sea spray number emission fluxes. Dependence of sea spray fluxes was investigated in different water masses (i.e. subantarctic, subtropical and frontal bloom) with contrasting biogeochemical properties across a temperature range from ambient (13-18°C) to 2°C, using seawater circulating in a plunging jet sea spray generator. We observed sea spray total concentration to increase significantly at temperatures below 8 °C, with an average 4-fold increase at 2°C relative to initial concentration at ambient temperatures. This temperature dependence was more pronounced for smaller size sea spray particles (i.e. nucleation and Aitken modes). Moreover, temperature dependence varied with water mass type and so biogeochemical properties. While the sea spray flux at moderate temperatures (8-11°C) was highest in frontal bloom waters, the effect of low temperature on the sea spray flux was highest with subtropical seawaters. The temperature dependence of sea spray flux was also inversely proportional to the seawater cell abundance of the cyanobacterium Synechococcus, which facilitated parameterization of temperature dependence of sea spray emission fluxes as a function of Synechococcus for future implementation in modelling exercises.

1 Introduction

In the open ocean, bursting bubbles generated by breaking waves cause particles to be ejected into the atmosphere, in the form of sea spray aerosols (SSA) that may influence climate either via scattering solar radiation (Schulz et al., 2006; Bates et al., 2006) or by forming cloud droplets (Pierce and Adams, 2006) or ice crystals (Burrows et al. 2013). Recent modelling studies have highlighted large knowledge gaps related to sea spray emissions, particularly with the submicron size and effect of organic

matter (Bian et al., 2019; Regayre et al., 2020). Sea spray emission fluxes mainly depend on wind speed which determines the

35 presence of breaking waves, with a threshold of 4 m s-1 above which sea spray is emitted to the atmosphere. Another important parameter is surface seawater temperature (SST), as the size of bubbles rising to the surface, as well as physical parameters such as the thickness of the breaking bubble films, depend on surface tension, viscosity and density which are all a function of seawater temperature. Also, organic matter in surface seawater influences the bubble bursting process, as organics may alter sea spray mass, number and size, and so affect sea spray cloud condensation nuclei (CCN) properties (Fuentes et al. 2010;

40 Sellegri et al. 2021). Number based emission fluxes are especially important for cloud formation as the CCN number is more important than mass for cloud properties. Fossum et al. (2018) calculate that for high wind speeds, sea salt number concentrations may contribute 100% of CCN concentrations at realistic marine boundary layer cloud supersaturations in the Southern Ocean.

A number of sea salt aerosol emission parameterizations have been developed but the resulting size-dependant sea spray fluxes

45 range over one order of magnitude or more (de Leeuw et al. 2007, Ovadnevaite et al. 2014), particularly for sizes lower than 150 nm or larger than 1 micron (Grythe et al. 2014). This large discrepancy in sea spray emission flux parameterizations may reflect the different methods used to measure fluxes in ambient air, and also the biophysical properties in different studies. For example, although fluxes are always parameterized as a function of wind speed, they are not always harmonized for a given seawater temperature or biological content, and when they do they show contradicting results.

50 Using in situ and remote sensing (AOD) measurements to constrain a global model, Jaeglé et al. (2011) derived a parametrization with sea spray flux increasing with temperature over the full temperature range investigated (0-30°C). Consistent with these observations Ovadnevaite et al. 2014 report a positive relationship between sea spray mass fluxes and SST, derived from observation of in-situ coastal sea spray aerosol concentrations and meteorological parameters. Also, Grythe et al. 2014 generated a similar positive linear relationship between sea spray mass and SST from a large data set of fixed station

55 and ship-borne aerosol measurements, using sodium and a source receptor approach combined with a model. Lastly, Liu et al. 2021 derive a SST dependence of sea-spray fluxes , expressed as sea spray mass for different wind speed ranges that agree with the previously mentioned trends. In summary, the majority of studies using ambient aerosol mass have identified a positive relationship between SSA and SST.

Laboratory experiments using plunging-jet sea-spray generator enable the study of the sea-spray number flux (as opposed to

60 sea spray mass) temperature dependence over different ranges of sea-spray size and also temperature. Usually, relationships derived from number concentration fluxes measurements in the laboratory, dominated by submicron sea-spray aerosols, differ considerably from those obtained from optical ambient measurements such as those described above. Martensson et al. (2003) provide two different temperature dependences of the sea-spray flux over the SST range 0-25°C: one for submicron sea spray, showing an increase of the flux with decreasing temperature, and one for the supermicron size range of sea spray with

65 increasing flux of sea spray with SST. Similar opposing behaviour between submicron and supermicron particles was reported

by Bowyer et al. 1990. Salter et al. (2014) also found differences in the sea-spray fluxes when considering small and larger sizes of sea spray, but they additionally showed different dependences either side of a temperature threshold of 10°C, i.e. increasing fluxes with increasing SST above 10°C and decreasing fluxes with increasing SST below this limit. Schwier et al. (2017) found an increase in submicron sea-spray fluxes with Mediterranean seawater at temperatures in the 22-29 °C, confirming the results from Salter et al. (2014). Recently, Christiansen et al. (2019) provided a detailed study on the impact of air entrainment, temperature. Their work confirmed the physical impact of temperature on synthetic seawater with an increase in sub-micrometer sea-spray aerosol with decreasing temperature below 6-10°C, and an increase of sub-micrometer sea-spray aerosol with increasing temperature above this range.

Temperature has an impact on seawater viscosity, density and surface tension, with all these parameters increasing when temperature decreases and also impacts on the evaporation rate of the bubble film. The combination of viscosity, density and surface tension changes may also affect the volume of air entrained in the seawater and the total volume and number of bubbles formed. Thorpe et al., (1992) used a numerical model that showed a significant decrease of the mean bubble concentration with increasing temperature, with a halving for every 10°C for bubbles with radii in the 10-150 μm range. However, Christiansen et al. 2019 reported little change with temperature in air entrainment flows via a plunging jet system over the temperature range -2 to 35°C, and Zabori et al. (2012) did not detect any change with temperature of the bubble size distribution in natural seawater over the range -2 to 10°C.

It appears from the large discrepancies between temperature dependences of the sea-spray flux derived from these different approaches that the factors controlling the SSA fluxes are not fully understood, and so not well conceptualized and represented. In their study, Forestieri et al. (2018) highlight that the seawater temperature sensitivity of SSA produced in plunging jet experiments differ greatly between synthetic and natural seawaters. Unlike experiments using synthetic salt solutions that show a monotonic increase of the sea-spray fluxes with seawater temperature, the dependence of sea-spray fluxes to temperature in natural seawaters showed substantial inconsistencies. The authors hypothesize that biological processes induce variations in the surface-active species in the seawater that drive changes in the sea-spray fluxes.

Surfactants influence the bubble bursting mechanism by decreasing or increasing bubble lifetime and size (Modini et al. 2013, Tyree et al. 2007). The presence of surfactant in seawater can cause a decrease in the average SSA size (Sellegri et al. 2006), and an increase or decrease of the number production flux of particles ejected (Tyree et al. 2007; Zábori, et al. 2012), depending on the type of surfactant. Surfactants in the seawater may originate from phytoplankton exudates in the form of dissolved organic matter (carboxylic acids, lipids, amino acids, carbohydrates, etc.) (Aluwihare and Repeta 1999; Barthelmeß and Engel 2022). Surfactant production has been demonstrated with healthy cells of different phytoplankton groups (Zutic et al, 1981) and also during zooplankton grazing on phytoplankton (Kujawinski et al, 2002). In Sellegri et al. (2021), it was shown that the SSA number production flux was a function of the nanophytoplankton cell abundances in surface seawater, for a given temperature. In the same study, sea-spray production fluxes were related to seawater fatty acid concentrations, and associated

with a change in seawater surface tension. A clear relationship between nanophytoplankton abundance, the release of labile organic matter and surface activity was also recently confirmed by Barthelmeß and Engel (2022). The role that surfactants

100   play in determining seawater surface tension and the resulting bubbles at low temperatures is however unclear and may depend on the nature of the surfactants present. To address these uncertainties we investigate the temperature dependence of sea-spray aerosols generated from natural seawater of contrasting water masses of the South-Western Pacific Ocean and relate this to the biogeochemical properties of the surface water.

2 Material and Methods

105   Measurements were performed during the Sea2Cloud voyage that took place in March 2020 east of New Zealand on board the R/V Tangaroa (Sellegri et al. 2022). Sea spray was continuously generated with a plunging jet system, as described in detail in Sellegri et al. (2022) and previously used in Schwier et al. 2015 and 2017, Trueblood et al. 2021, Freney et al. 2021 and Sellegri et al. 2021. The sea-spray generation system was operated at constant jet flow rate, corresponding to an air entrainment rate of 0.75 L min^{-1}. The system reproduces sea-spray size distributions of similar shape to those reported for other plunging

110   jet devices (Fuentes et al. 2010). The system was fed continuously with seawater sampled from a depth of ~6 m by the underway seawater supply. Using a 50 L temperature-controlled reservoir, temperature gradients between 2°C and 15°C were applied to the seawater over approximately 1 hour, with an initial decreasing temperature ramp, followed by an increasing temperature ramp. Temperature experiments were performed every morning around 11 am from 18/03/20 to 26/03/20, with an additional experiment in the afternoon of 26/03/20.

115   The total generated sea-spray concentration was monitored using a MAGIC Condensation Particle Counter (CPC), with size distribution measured using a Differential Mobility Particle Sizer (DMPS) scanning from 10 to 500 nm in diameter, and a Waveband Integrated Bioaerosol Sensor (WIBS) for diameters ranging from 500 nm up to 4500 nm. Sea-spray chemical composition was followed online using an Aerosol Chemical Speciation Monitor (ACSM), and its fluorescence properties using the WIBS.

120   Similar to Sellegri et al. (2021), hereafter referred to as SELL21, the concentration of > 100 nm particles was used as a proxy for CCN concentration, with FCCN corresponding to the flux of > 100 nm SSA. FCCN was first calculated from the > 100 nm SSA number concentration, flush air flow and water surface of the tank, and then normalized to a 10 m elevation wind speed (U_{10}) of 9 m s-1, using the same approach as described in SELL21, to allow for the comparison of the fluxes between the different experiments. Briefly, this harmonization procedure is based on a second calculation of the fluxes which involves

Atmospheric
Chemistry
and Physics
Discussions
Open Access
EGU

125   the volume of air entrained by the plunging jets in the SSA generator, and also uses the expression of Long et al. (2011) which relates the volume of air entrained in a plunging air system in the atmosphere to U_{10}.

The seawater surface tension was measured from the ship-board underway seawater line at 08:00, 12:00, 16:00 and 20:00 NZDT using the bubble lifetime method with a Dynotester along a temperature gradient from 2 to 15°C. The temperature gradient for surface tension measurements was achieved by first freezing 25 ml seawater sampled in Falcon tubes, with surface

130   tension measured while the sample slowly warmed to ambient temperature; this took less than one hour which limited the time for any seawater biogeochemistry changes to occur.

For the analysis of the seawater biogeochemical properties, discrete water samples were collected from the ships underway seawater line into an acid-cleaned 10L plastic carboy at 4 hr intervals (00:00, 04:00, 08:00, 12:00, 16:00, 20:00 NZDT). Seawater aliquots were taken from the carboy for chlorophyll a (Chl-a), macronutrients, Total Organic Carbon (TOC) and

135   microbial community composition (flow cytometry and microscopy).

For chlorophyll-a analysis, 250 ml of seawater was filtered through 47 mm 0.2 µm polycarbonate filters and the pigment retained on the filters was extracted with 90% acetone and measured by spectrofluorometry using a Varian Cary spectrofluorometer. For macronutrient analysis, 250 ml of seawater was filtered through 25 mm GF/F filters into 250ml plastic bottles, and nutrients (Ammonia, Nitrate and Nitrite, Dissolved Reactive Phosphorus, and Silica) measured on a SEAL AA3

140   Autoanalyser (Law et al. 2011). The TOC content of samples was analyzed by catalytic oxidation (TOC-VCSH analyser, Shimadzu) after the modified protocol of Sugimura and Suzuki (1988) (Engel and Galgani, 2016). Samples were filled into 20 ml pre-combusted glass ampules (8 h at 500°C), acidified with 20 µl 32% HCl, subsequently sealed and stored at 4°C until the analysis.

For Flow-cytometry, duplicated 1.5 mL seawater samples were preserved with a solution containing glutaraldehyde (Naik,

145   S.M. and Anil, 2017), flash frozen and stored at -80°C. Samples were analyzed with a BD FACSCalibur instrument and Synechococcus and picoeukaryote cells quantified using TrucountTM beads (Becton Dickinson, Mountain 108 View, CA), as described in Hall and Safi (2001). Total numbers of heterotrophic bacteria, eukaryotic nanophytoplankton (2-20µm) and prokaryotic and eukaryotic picophytoplankton (<2 µm) were determined by flow cytometry using a BD Accuri™ C6 Plus instrument (BD Biosciences). Bacteria samples were stained with Sybr Green II and a minimum of 20,000 bacteria events

150   were analysed using SSC vs FL1 plot. For the phytoplankton analyses 250 uL of sample was analysed and the eukaryotic plankton populations were identified using a SSC vs FL3 plot while the prokaryotic picoplankton (Synechococcus sp.) population was identified using a FL1 vs FL2For microscopy analysis, 500 ml of seawater was fixed to 1% with Lugol's iodine

solution and phytoplankton community composition and cell numbers for species >5 µm were determined using optical microscopy, as described in Safi et al. (2007) and references therein.

3 Results and discussion

3.1. General feature of the seawaters investigated

The region east of the New Zealand South Island provides an ideal platform for investigating variability in SSA and its relationship with surface ocean biogeochemistry due to the close proximity of different water masses (Law et al, 2018). The Sea2Cloud voyage occupied frontal water from 17/03/2020 11:00-20 /03/2020 17:00, and then subantarctic water (SAW) until 24/03/2020 4:00, then subtropical waters (STW) until 25/03/2020 8:00, and finally mixed-shelf water to 27/03/2020.The Subtropical Front which runs along 43oS-43.5oS separates subtropical and subantarctic water and is evident year-round in ocean colour images as an area of elevated phytoplankton biomass relative to the low biomass water masses either side. The subtropical water north of the Front is warmer and saltier, relative to the colder, fresher, subantarctic water, with lower dissolved inorganic nutrients, particularly nitrogen and TOC. This variation in physical properties and nutrient availability results in different biological communities in the three water masses, with the Front characterized by blooms of different phytoplankton groups in spring and summer (Delizo et al., 2007; Law et al, 2018). Frontal waters contained higher cell abundances of nanophytoplankton (2-20 µm) than any other water masses sampled during the voyage, whereas cell abundances of the picoplankton (<2 um) *Synechococcus* were conversely higher in subantarctic and mixed/shelf water relative to frontal water (Figure 1). Diatom abundance was correlated with nanophytoplankton cell abundances (R^2=0,57, p<0.01). Differences in biological communities subsequently influence biogeochemical properties of these water masses resulting in differential effects upon aerosol precursors (Law et al, 2018; Sellegri et al, 2022).

3.2. Sea-spray fluxes at moderate ambient temperatures

The time series of the SSA flux measured at ambient SST (13-18 °C) are reported in Figure 1d. We observed that the SSA flux decreased from biologically-rich frontal waters at the start of the campaign to subantarctic seawaters that contained lower phytoplankton abundance, as indicated by the nanophytoplankton and diatoms (Fig. 1a and 1b). In Sellegri et al. (2021), a relationship was found between the flux of SSA >100 nm in size (the CCN fraction of sea spray at 0.2% supersaturation, F_{CCN}) with the nanophytoplankton cell abundance (NanoPhyto). Recently, Dall'Osto et al. (2022) also found increased SSA number production fluxes from nanophytoplankton-rich seawater but did not quantify the SSA flux-to-nanophytoplankton cell abundance relationship. Figure 2 presents this relationship between F_{CCN} and NanoPhyto for the Sea2Cloud data in comparison with datasets from other regions (SELL21). NanoPhyto during Sea2Cloud were higher on average and spanned a larger range (1490±732 cells mL^{-1}) than in oligotrophic Mediterranean waters (546±148 cells mL-1) and springtime Arctic waters in which NanoPhyto were almost absent (4.2±4.3 cells mL-1), but were lower than in a nutrient-enriched mesocosm experiment in New Zealand coastal waters (4880±2390 cells mL-1). When combining these five datasets, the F_{CCN} showed a weaker dependence

Atmospheric
Chemistry
and Physics
Discussions
Open Access
EGU

than reported in SELL21 but still confirmed the linear dependence of F_{CCN} on NanoPhyto, with a significant correlation (R^2 = 0.78, p<0.05). The coefficients of the revised fit differ only slightly to SELL21 with a greater statistical significance than for the individual datasets (R^2 = 0.78 vs 0.31 for the Sea2Cloud dataset). Following the SELL21 approach, the relationship was reformulated with F_{CCN} expressed as a function of both NanoPhyto and $F_{CCN-inorg}$ with $F_{CCN-inorg}$ corresponding to F_{CCN} in the absence of biological activity (i.e. solely inorganic chemical components), and hence shown as the intercept of the y axis (2.41×10^5 m^{-2} s^{-1}):

$$F_{CCN} = F_{CCN-inorg} \times (1 + 9.7 \ 10^{-3} \times NanoPhyto) \qquad (1)$$

The primary motivation for this reformulation was to allow a simpler implementation of the parameterisation in models that already include the calculation of $F_{CCN-inorg}$. As a reminder, the fluxes used to derive Eq. (1) were normalized to $U_{10} = 9$ m s^{-1} and SST=15°C. We cannot exclude that the dependence of F_{CCN} on NanoPhyto changes for different wind regimes, but not having this information we assume here that Eq. (1) applies to the calculation of F_{CCN} regardless of U_{10}.

Figure 1d also shows the time series of surface tension of the seawater samples at 15°C, that closely follow the SSA fluxes at ambient temperature close to 15°C. Recently, Barthelmeß and Engel (2022) also reported a dependence of surfactant release to nanophytoplankton in the Baltic Sea. Higher surface tension induces higher bubble lifetime and therefore thinner bubble films due to increased drainage and increased evaporation. On bursting, thinner bubble films generate a higher number of smaller droplets (Lhuissier and Villermaux, 2012; Poulain and Bourouiba, 2018).

3.3.   Temperature dependence of total spray emission fluxes

For all low temperature gradient experiments we observed an increase in sea-spray total number fluxes with decreasing temperature in all seawater types (Figure 2). There was a change in the sea spray flux gradient with little or no gradient above 8-10°C and a sharp increase below these temperatures. This feature was previously observed by Salter et al. (2014) with inorganic seawater, and also Hultin et al. (2011) using Baltic seawater and a sea spray generation system similar to this study, although Hultin et al. (2011) reported a SSA emission flux increase with decreasing temperature already below 12°C.

Surface tension of the seawater, measured as a function of temperature, showed a clear increase with decreasing temperature, and also large differences between water types for a given temperature, including >8 °C (Figure 4).The temperature dependence of surface tension (Figure 4) did not follow the same trend as the temperature dependence of the SSA flux (Figure 3), with a relatively monotonic decrease of surface tension with increasing temperature extending above 8 °C, in contrast to the behaviour of sea-spray fluxes. Also, higher surface tension at low temperatures did not correspond to higher sea-spray

Atmospheric
Chemistry
and Physics
Discussions
Open Access
EGU

fluxes at these temperatures. This suggests that while surface tension seems to influence sea-spray emission in the 8-15°C temperature range, it does not fully explain observed changes in SSA fluxes below temperatures of 8 °C alone.

In order to decouple the biological impact on SSA fluxes at temperatures in the 8-15 °C range from the influence of lower temperature, we normalized the sea-spray flux at a given temperature (F_T) with the sea-spray flux at 8 °C (F_8). As presented in
215 Figure 5, this enabled evaluation of the relative increase of the corresponding sea-spray flux with respect to F_8 for a given temperature in the same experiment. The normalization also facilitates comparison of the flux-temperature relationship with those observed in the literature.

The best fit for the normalized sea-spray flux temperature dependence is a polynomial fit of the second order of the following form:

220
$$\frac{F_T}{F_8} = p1 * T^2 + p2 * T + p3 \tag{2}$$

When fitting each daily temperature experiment individually, we obtain a time series of coefficients p_1 p_2 and, as p_1 and p_2 are highly correlated to p_3, it can be expressed as a function of $p3$ in a final relationship:

$$\frac{F_T}{F_8} = \boldsymbol{p3} + (\boldsymbol{0,0382} - \boldsymbol{0,243p3}) * \boldsymbol{T} + (\boldsymbol{0,0138p3} - \boldsymbol{0,02}) * \boldsymbol{T^2}$$

225
$$\tag{3}$$

When the fit is performed on all data together, p_3=4.343. Therefore, on average, for a temperature of 1 °C, the sea-spray flux is increased by a factor of approximately 4 relative to the flux at 8 °C. This parameterization is only valid for temperatures below 8 °C whereas fluxes can be considered independent of temperature above 15°C. The temporal variability of the fitting parameter p_3 of equation (3) can be studied as a function of the seawater biogeochemical properties. We searched for
230 correlations between p_3 and the different phytoplankton communities (including nanophytoplankton, flagellates, diatoms, and dinoflagellates), bacteria or biogeochemical variables (TOC, amino acids and carbohydrates). No relationship was found except a significant anticorrelation with *Synechococcus* cell abundance (R^2=0,72, n=10, p< 0.00001), with the following relationship showing the temperature dependence of SSA as a function of *Synechococcus* cell abundances expressed in cells ml^{-1}:

235   p_3=6.54-2.10^{-5}*Synechococcus   (4)

The reason for this anticorrelation is not clear. *Synechococcus* spp. is an autotrophic prokaryote (bacterium) which is ubiquitously present throughout oceanic regimes (Zwirglemaier et al., 2007; Six et al., 2021). *Synechococcus*-derived dissolved organic matter (SOM) is released via secretion, natural cell death, viral lysis, and predation (Jiao et al., 2010; Fiore et al., 2015;

Xiao et al., 2020) and contributes to the marine dissolved organic matter pool (Jiao et al., 2011; Gontikaki et al., 2013). The
240 presence of *Synechococcus* spp. increased organic carbon content in SSA particles relative to artificial seawater by a factor of
34 (Moore et al., 2010). Rich in nitrate, the largest proportion of SOM is labile and quickly consumed by heterotrophic bacteria,
which release exoenzymes to cleave biopolymers (Christie-Oleza et al., 2015; Zheng et al., 2021). Poulain and Barouiba,
(2018) suggest that the presence of heterotrophic bacteria and their lysates induced the prolongation of lifetime and thinning
of the bubble surface, which in turn increases the formation rate of smaller aerosol particles (Section 3.4).

245 The anticorrelation with *Synechococcus* that we observe could indicate a release of SOM during their decay arising from
mortality, viral lysis or predation, rather than secretion (which would be positively related to *Synechococcus* cell abundance).
Surfactant release was also anticorrelated to *Synechococcus* abundance in the Baltic Sea, and was interpreted as grazing of
nanophytoplankton on *Synechococcus* cells (Barthelmeß and Engel, 2022). In theory, we could thus explain the enhanced SSA
flux within the lower temperature regimes by the presence of biosurfactants released (a) directly by *Synechococcus* during cell
250 lysis, or (b) indirectly by related heterotrophic prokaryotes. Bacterial abundance does not represent their metabolic activity or
secretion rate, as bacterial cells can also remain inactive (Lebaron et al., 2001), and so a lack of correlation with bacterial
abundance does not necessarily falsify hypothesis (b). However, we cannot exclude that the observed anticorrelation with
Synechococcus is coincidental rather than causal.

Next, we investigate if seawater biogeochemistry also influences the size of SSA emissions at low temperatures.

255 ## 3.4.   Size segregated sea-spray fluxes

The aerosol size distribution in the 10-4000 nm range, from merged SMPS and WIBS size distributions, was normalized to
the total sea-spray concentrations in order to investigate changes in size distribution shape rather than number (studied section
2.3). These were averaged over two contrasted temperatures ranges, 2-3 °C and 7-9 °, and fitted with single lognormal modes
(Figure 6). In the moderate temperature range (7-9°C), we found 4 modes in the submicron range and two modes in the
260 supermicron range that best characterize the sea-spray aerosol, with characteristics summarized in Table 1. These
characteristics are very similar to that reported for sea spray generated with the same device using Mediterranean water
(Schwier et al. 2017, Sellegri et al. 2021), and also to sea-spray size distributions generated with other jet-based approaches
that showed a dominant mode centred around 100 nm (Sellegri et al. 2006, Fuentes et al. 2010; Christiansen et al. 2019).
Christiansen et al. 2019 report that the shape of the particle size distributions and mode contributions are only slightly affected
265 by addition of algae. We also find that the variability of the SSA size distributions at moderate temperature is low between
samples, as also pointed out by Sellegri et al. (2021) for seawater from various geographical origins.

When comparing size distributions in the two temperature ranges, we find that the shape of the size distribution is not preserved
at 2-3 °C relative to 7-9 °C. The fraction of the smaller particle sizes (nucleation and Aitken modes) relative to the total sea-

270 spray concentration increases at cold temperatures compared to warmer ones, whereas it decreases for the largest sizes. The average ratio of number concentrations of SSA smaller than 50 nm to the total SSA concentration was 0.19 ± 0.03 in the 7-9 °C range, while it was 0.35 ± 0.04 in the 2-3 °C range, indicating that the size distribution variation due to low temperature significantly exceeded the variability of size distributions due to seawater types at moderate temperature.

275

In order to quantify changes of sea-spray concentrations per size range, we calculated modal concentrations by summing particle concentrations in particle size bins within each mode: nucleation mode (11 nm - 15 nm), Aitken mode (20 nm - 44 nm), accumulation mode 1 (68 nm - 142 nm), accumulation mode 2 (267 nm - 430 nm) and coarse mode (710 nm - 4485 nm). The relation to temperature of each modal concentration normalized to its concentration at 8-10 °C was then plotted for each
280 individual mode and linearly fitted over the 3 to 10 °C temperature range for each experiment. A polynomial fit, as with equation (2), could not be obtained and instead a linear fit provided the optimal fit given the small number of data points obtained with a 13 min scanning time necessary for each size distribution. Statistics on the relative increase of each modal concentration per SST degree, relative to its 8-10 °C modal concentration are shown Figure 7.

285 We observe that sea-spray concentrations in all modal sizes increased with decreasing temperature, but the sea-spray concentrations in the nucleation mode on average show the largest relative increase, followed by concentrations in the Aitken mode. Small particles are therefore most sensitive to temperature of the ocean surface water. Christiansen et al. (2019) also observed that the relative amount of small (<40 nm) particles increased at the coldest temperatures using synthetic seawater, indicating that this is at least partly due to physical parameters. However, contrary to our observations they observed that larger
290 (>300 nm) particles increased at the lowest temperatures. Using natural seawaters from a fjord in the Arctic, Zabori et al. (2012) found that the ratio of smaller (180 nm) to larger (570 nm) sea-spray particles increased at seawater temperatures colder than 3°C relative to temperatures above 3°C, which is consistent with our observations.

One potential explanation is that the bubble film is stabilized by surfactant so that when it bursts it generates larger amounts
295 of smaller film drops whose residues are smaller (Lhuissier and Villermaux 2012; Poulain and Bourouiba, 2018). Additionally, when the main bubble bursts at the air-sea interface, numerous daughter bubbles of smaller diameter form at the edge of the main bubble (Bird et al. 2010; Millet et al. 2021), which may be the origin of additional drops of smaller sizes ejected to the atmosphere. The formation of daughter bubbles increases with the ratio of density to viscosity, and further with the ratio of viscosity to surface tension. All of these variables increase with decreasing temperature, but it is difficult to quantify how their
300 ratio evolves in the presence of unknown active chemicals.

4 Conclusions

The significant increase of SSA flux with decreasing temperature is consistent with observations from laboratory-based experiments on synthetic and natural seawaters (Hultin et al. 2011; Zabori et al. 2012; Salter et al. 2014; Christiansen et al. 2019), but not with the temperature dependence of sea spray fluxes assessed from ambient concentrations (Jaegle et al. 2011;

305 Grythe et al. 2014). The reported temperature dependences from ambient concentrations were performed using either optical depth measurements (Jaegle et al. 2011) or sodium containing particles (Grythe et al. 2014), mostly represented by large accumulation mode particles that do not necessarily follow the same trends as the SSA number concentrations, mostly represented by smaller particles. We do find that larger SSA particle fluxes are not as sensitive to temperature as smaller ones. Also, in ambient air, it is difficult to discriminate between primary sea-spray production and secondary aerosol formation that

310 either forms new particles or grows pre-existing particles, and may also be dependent on temperature. Therefore, the apparent contradiction between laboratory-based and ambient air sea-spray fluxes studies may be due to these two types of studies addressing differing aerosol sizes and processing/mixing states.

Comparison with results obtained from synthetic seawater in the literature is not straightforward as different conclusions are

315 obtained in different studies. For example, Forestieri et al. 2018 report a monotonic increase of sea spray with increasing temperature, while Christiansen et al. (2019) reports a minimum in the sea-spray flux in the range 6-10°C, with both studies using synthetic sea spray and plunging jet systems, over the same range of temperature. As noted by Forestieri et al. (2018), variability between repeated experiments in their study (and so between different studies) could result from trace impurities of surfactants in the commercial synthetic salt solutions. Christiansen et al. (2019) also report a baseline TOC content of around

320 1.2 mg L^{-1} in a 35 g L^{-1} sigma sea salt solution, corresponding to <0.003% by mass and also the amount of TOC found in frontal waters during Sea2Cloud. Moreover, our sample with the lowest temperature dependence (March 18th, high Chl-a and TOC frontal seawaters) compares well with the temperature dependence flux model from Salter et al. (2014) and with synthetic seawater reported by Christiansen et al. (2019), while our highest temperature dependence samples (March 23rd and 24th, low Chl-a and TOC subantarctic seawaters) compare well with the temperature dependence experiments performed by Zabori et

325 al. (2012) using arctic seawaters of different origins (Figure 5). This indicates that neither Chl-a nor TOC are a good proxy for predicting the sea-spray flux temperature dependence.

Nanophytoplankton abundance was a major determinant of sea-spray number fluxes for sizes larger than 100 nm at moderate temperatures (SELL21), which was attributed to fatty acid concentration and surface tension effects. This is further supported

330 in the present study, although the relationship to nanophytoplankton is not as strong as in SELL21. Here we show that the seawater temperature effect is inversely dependent on another phytoplankton group, the genus *Synechococcus* spp, which, if not coincidential, could indicate a link to SOM release during decay. However, there is heterogeneity within the *Synechococcus* genus and within the picoplankton in general, Our results might be specific to *Synechococcus* spp. population

of the South-Western Pacific Ocean and further work is required to investigate if the present relationship is applicable at a
335   larger regional scale. In addition, more work is required to investigate the process by which *Synechococcus spp.* are related to
the release of organic matter that specifically influences SSA flux at low temperature.

The dependence of SSA fluxes on water temperature is highest for nucleation and Aitken mode particles, but remains high for
SSA sizes of the 100-200 nm size, which dominate the total SSA flux and are active as CCN. Consequently, this should
340   influence the seasonal variability of sea-spray particles in cold surface waters such as in the Southern Ocean. It may be also
be relevant with respect to the cool-skin effect at the ocean-atmosphere interface. Average surface cooling by 0.2 K at global
mean wind regimes (6 m sec^{-1}) relative to depths >1cm (Donlon et al., 2002) may occur and may be greater under lower wind
regimes or at night (Donlon et al., 2002, Marmarino and Smith, 2006). As SSA fluxes are generated at this interface they are
influenced by the biophysical conditions encountered i.e. often characterized by an enrichment in biosurfactants (Wurl et al.,
345   2011).

The IPCC report estimates an increase in average ocean surface temperature by 2.5 ° C by 2100, with consequences for marine
biology (Bindoff et al. 2019). Ocean warming is expected to expand the distribution range and cell abundance of
Synechococcus (Morán et al., 2010; Flombaum et al., 2013). Our results indicate that higher ambient temperatures and
Synechococcus abundance would lead to weaker sea-spray flux number concentrations at low temperatures with a combined
350   effect potentially additive or even synergitic compared to each of these individual effects. However, higher temperatures and
an increased release of labile SOM could cause an effect on bacterial metabolism (Piontek et al., 2015) that potentially favours
the secretion of biosurfactants by heterotrophic bacteria. Potential changes in the abundance of *Synechococcus* spp. in response
to temperature changes associated with climate change, and the resulting impact on CCN fluxes to the atmosphere and cloud
formation can only be investigated using regional models run under future climate conditions. The quantification of process-
355   based relationships between seawater biogeochemistry and sea-spray cloud forming properties derived from the present study
should enable improved actual simulations of cloud formation over the oceans of the Southern Hemisphere.

Author contribution

KSe and CL designed the Sea2Cloud voyage. KSe designed the experiments with the contribution of NB and MH and KSe
and JT carried them out. TB, AC, KSa, SD and WD sampled seawater for biogeochemical analysis and AC, KSa, SD and KT
360   analysed sampled. AE supervised the work of TB. EF and CR contributed to aerosol measurement analysis. KSe prepared the
manuscript with contributions from all co-authors.

Atmospheric
Chemistry
and Physics
Discussions

Aknowledgements

References

Alpers,W.   "Surface   Films".   In: Elsevier.
370 Aluwihare, LI et DJ Repeta (1999). "A comparison of the chemical characteristics of oceanic DOM and extracellular DOM produced by marine algae". In : Marine Ecology Progress Series 186, p105-117, 2019

Andreae, M. O. (1985). "The Emission of Sulfur to the Remote Atmosphere : Background Paper". In : The Biogeochemical Cycling of Sulfur and Nitrogen in the Remote Atmosphere. Sous la dir. de James N. Galloway et al. Dordrecht : Springer Nether- lands, p. 5-25. isbn : 978-94-009-5476-2. doi : 10.1007/978-94-009-5476-2_2. url
375 : https://doi.org/10.1007/978-94-009-5476-2_2.

Barthelmeß, T. and Engel, A.: How biogenic polymers control surfactant dynamics in the surface microlayer: Insights from a coastal Baltic Sea study, Biogeosciences Discuss. [preprint], https://doi.org/10.5194/bg-2022-128, in review, 2022

Bates, T. S., et al. (2006), Aerosol direct radiative effects over the northwest Atlantic, northwest Pacific, and North
380 Indian Oceans: Estimates based on in-situ chemical and optical measurements and transport modelling, Atmos. Chem. Phys., 6, 1657–1732.

Bian, H., Froyd, K., Murphy, D. M., Dibb, J., Darmenov, A., Chin, M., Colarco, P. R., da Silva, A., Kucsera, T. L., Schill, G., Yu, H., Bui, P., Dollner, M., Weinzierl, B., and Smirnov, A.: Observationally constrained analysis of sea salt aerosol in the marine atmosphere, Atmos. Chem. Phys., 19, 10773–10785, https://doi.org/10.5194/acp-19-
385 10773-2019, 2019.

Bird, James C et al.. "Daughter bubble cascades produced by folding of ruptured thin films". Nature 465.7299, p. 759-762, 2010.

Bindoff, Nathaniel L et al. (2019). "Changing ocean, marine ecosystems, and dependent communities". In : IPCC
390 special report on the ocean and cryosphere in a changing climate, p. 477-587.

Bowyer, P. A., Woolf, D. K., and Monahan, E. C.: Temperature dependence of the charge and aerosol production associated with a breaking wave in a whitecap simulation tank, J. Geo- phys. Res.-Oceans, 95, 5313–5319, doi:10.1029/JC095iC04p05313, 1990. 16107

395 Burrows, S. M., Hoose, C., Pöschl, U., and Lawrence, M. G.: Ice nuclei in marine air: biogenic particles or dust?, Atmos. Chem. Phys., 13, 245–267, https://doi.org/10.5194/acp-13-245-2013, 2013.

Christiansen, Sigurd et al. (2019). "Sea spray aerosol formation : Laboratory results on the role of air entrainment, water temperature, and phytoplankton biomass". In : Environmental science & technology 53.22, p. 13107-13116.

Christie-Oleza, J. A., Scanlan, D. J., & Armengaud, J. (2015). "You produce while I clean up", a strategy revealed by exoproteomics during Synechococcus-Roseobacter interactions. Proteomics, 15(20), 3454–3462.
400 https://doi.org/10.1002/pmic.201400562

Dall'Osto M, Vaque ́D, Sotomayor-Garcia A, Cabrera-Brufau M, Estrada M, Buchaca T, Soler M, Nunes S, Zeppenfeld S, van Pinxteren M, Herrmann H, Wex H, Rinaldi M, Paglione M, Beddows DCS, Harrison RM and Berdalet E (2022) Sea Ice Microbiota in the Antarctic Peninsula Modulates Cloud-Relevant Sea Spray Aerosol Production. Front. Mar. Sci. 9:827061. doi: 10.3389/fmars.2022.827061

405 de Leeuw, G., E. L. Andreas, M. D. Anguelova, C. W. Fairall, E. R. Lewis, C. D. ODowd, M. Schulz, and S. E. Schwartz (2011), Production flux of sea spray aerosol, Rev. Geophys., 49(RG2001), 349.

Delizo, L., Smith, W. O., and Hall, J.: Taxonomic composition and growth rates of phytoplankton assemblages at the Subtropical Convergence east of New Zealand, J. Plankton Res., 29, 655– 670, https://doi.org/10.1093/plankt/fbm047, 2007.

410 Donlon, C. J., Minnett, P. J., Gentemann, C., Nightingale, T. J., Barton, I. J., Ward, B., & Murray, M. J. (2002). Toward improved validation of satellite sea surface skin temperature measurements for climate research. Journal of Climate, 15(4), 353–369. https://doi.org/10.1175/1520-0442(2002)015<0353:TIVOSS>2.0.CO;2

Engel, A., & Galgani, L. (2016). The organic sea-surface microlayer in the upwelling region off the coast of Peru and potential implications for air-sea exchange processes. Biogeosciences, 13(4), 989–1007.
415 https://doi.org/10.5194/bg-13-989-2016

Flombaum, P., Gallegos, J.L., Gordillo, R.A., Rincón, J., Zabala, L.L., Jiao, N., Karl, D.M., Li, W.K., Lomas, M.W., Veneziano, D. and Vera, C.S., 2013. Present and future global distributions of the marine Cyanobacteria Prochlorococcus and Synechococcus. Proceedings of the National Academy of Sciences, 110(24), pp.9824-9829.

Forestieri, SD et al. (2018). "Temperature and composition dependence of sea spray aerosol production". In : Geophysical Research Letters 45.14, p. 7218-7225.
420

Fuentes, E et al. (2009). "Laboratory-generated primary marine aerosol via bubble- bursting and atomization". In : Atmospheric Measurement Techniques Discussions 2.5, p. 2281-2320.

Fuentes, E., Coe, H., Green, D., de Leeuw, G., and McFiggans, G.: On the impacts of phytoplankton-derived organic matter on the properties of the primary marine aerosol – Part 1: Source fluxes, Atmos. Chem. Phys., 10,
425   9295–9317, https://doi.org/10.5194/acp-10-9295-2010, 2010.

Geider, Richard et Julie La Roche (2002). "Redfield revisited : variability of C : N : P in marine microalgae and its biochemical basis". In : European Journal of Phycology 37.1, p. 1-17.

Grythe, Henrik et al. (2014). "A review of sea-spray aerosol source functions using a large global set of sea salt aerosol concentration measurements". In : Atmospheric Chemistry and Physics 14.3, p. 1277-1297.

430   Hall, J.A. and Safi, K., 2001. The impact of in situ Fe fertilisation on the microbial food web in the Southern Ocean. Deep Sea Research Part II: Topical Studies in Oceanography, 48(11-12), pp.2591-2613.

Hultin, K. A. H., Krejci, R., Pinhassi, J., Gomez-Consarnau, L., Mårtensson, E. M., Hagström, A., and Nilsson, E. D.: Aerosol and bacterial emissions from Baltic seawater, Atmos. Res., 99, 1–14, doi:10.1016/j.atmosres.2010.08.018, 2011. 16088, 16106, 16107

435   Jaeglé, L et al. (2011). "Global distribution of sea salt aerosols : new constraints from in situ and remote sensing observations". In : Atmospheric Chemistry and Physics 11.7, p. 3137-3157.

Kujawinski, E.B., Farrington, J.W. and Moffett, J.W., 2002. Evidence for grazing-mediated production of dissolved surface-active material by marine protists. Marine chemistry, 77(2-3), pp.133-142.

Law, C.S., Smith, M., Stevens, C., Abraham, E.R., Ellwood, M., Hill, P., Nodder, S., Peloquin, J., Pickmere, S.,
440   Safi, K., Walkington, M., 2011. Did dilution limit the phytoplankton response to iron addition in HNLCLSi Sub-Antarctic waters during SAGE? Deep-Sea Res II, 58:786–799.

Law CS, Smith MJ, Harvey MJ, Bell TG, Cravigan LT, Elliott FC, Lawson SJ, Lizotte M, Marriner A, McGregor J, Ristovski Z, Safi KA, Saltzman ES, Vaattovaarra P, Walker CF. 2017. Overview and preliminary results of the Surface Ocean Aerosol Production (SOAP) campaign. Atmospheric Chemistry Physics, 17(22): 13645--13667,
445   doi: 10.5194/acp-17-13645-2017

Lebaron, P., Servais, P., Agogué, H., Courties, C., & Joux, F. (2001). Does the High Nucleic Acid Content of Individual Bacterial Cells Allow Us to Discriminate between Active Cells and Inactive Cells in Aquatic Systems? Applied and Environmental Microbiology, 67(4), 1775–1782. https://doi.org/10.1128/AEM.67.4.1775-1782.2001

450 Lhuissier, H. and E. Villermaux, « Bursting bubble aerosols", Journal of Fluid Mechanics , Volume 696, pp. 5 – 44, https://doi.org/10.1017/jfm.2011.418, 2012.

Liu, S. Cheng-Cheng Liu, Karl D. Froyd, Gregory P. Schill, Daniel M. Murphy, T. Paul Bui, Jonathan M. Dean-Day, Bernadett Weinzierl, Maximilian Dollner, Glenn S. Diskin, Gao Chen, and Ru-Shan Gao, Sea spray aerosol concentration modulated by sea surface temperature, PNAS, 2021 Vol. 118 No. 9 e2020583118, https://doi.org/10.1073/pnas.2020583118 , 2021

455 Long, MS et al. (2014). "Light-enhanced primary marine aerosol production from biologically productive seawater". In : Geophysical Research Letters 41.7, p. 2661-2670.

Marmorino, G. O., & Smith, G. B. (2006). Reduction of surface temperature in ocean slicks. Geophysical Research Letters, 33(14), 1–5. https://doi.org/10.1029/2006GL026502 Marmorino, G. O., & Smith, G. B. (2006). Reduction of surface temperature in ocean slicks. *Geophysical Research Letters*, *33*(14), 1–5. 460 https://doi.org/10.1029/2006GL026502

Martensson, E.M., E.D. Nilsoon, G de Leeuw, L.H. Cohen and H.-C. Hansson, "Laboratory simulations and parameterization of the primary marine aerosol production"; J. Geophys. Res., 108, doi: 10.1029/2002JD002263, 2003

465 Miguet,J., Rouyer, F. and Rio, E. The Life of a Surface Bubble. Molecules 2021, 26, 1317. https://doi.org/10.3390/molecules26051317

Modini, R. L. , L. M. Russell, G. B. Deane, & M. D. Stokes, Effect of soluble surfactant on bubble persistence and bubble-produced aerosol particles, *Journal of Geophysical Research*, **118**, 1388–1400. https://doi.org/10.1002/jgrd.50186, (2013).
470

Moore, M. J. K., Furutani, H., Roberts, G. C., Moffet, R. C., Gilles, M. K., Palenik, B., & Prather, K. A. (2011). Effect of organic compounds on cloud condensation nuclei (CCN) activity of sea spray aerosol produced by bubble bursting. Atmospheric Environment, 45(39), 7462–7469. https://doi.org/10.1016/j.atmosenv.2011.04.034

475 Morán, X., Lopez-Urrutia, A., Calvo-Díaz, A., and Li, W. K. W. (2010). Increasing importance of small phytoplankton in a warmer ocean. Glob. Chang. Biol. 16, 1137–1144. doi: 10.1111/J.1365-2486.2009.01960.X

Naik, S.M. and Anil, A.C., 2017. Long-term preservation of Tetraselmis indica (Chlorodendrophyceae, Chlorophyta) for flow cytometric analysis: Influence of fixative and storage temperature. Journal of microbiological methods, 139, pp.123-129.

480   Napolitano, Guillermo E et al. (1997). "Fatty acids as trophic markers of phytoplankton blooms in the Bahia Blanca estuary (Buenos Aires, Argentina) and in Trinity Bay (Newfoundland, Canada)". In : Biochemical Systematics and Ecology 25.8, p. 739-755.

O'Dowd, Colin D et al. (2004). "Biogenically driven organic contribution to marine aerosol". In : Nature 431.7009, p. 676-680.

485   Ovadnevaite, J et al. (2014). "A sea spray aerosol flux parameterization encapsulating wave state". In : Atmospheric Chemistry and Physics 14.4, p. 1837-1852.

Pierce, J. R., and P. J. Adams (2006), Global evaluation of CCN formation by direct emission of sea salt and growth of ultrafine sea salt, J. Geophys. Res., 111, D06,203, doi:10.1029/2005JD006186.

Piontek, J., Sperling, M., Nöthig, E. M., & Engel, A. (2015). Multiple environmental changes induce interactive
490   effects on bacterial degradation activity in the arctic ocean. Limnology and Oceanography, 60(4), 1392–1410. https://doi.org/10.1002/lno.10112

Poulain, S and L. Bourouiba, Biosurfactants Change the Thinning of Contaminated Bubbles at Bacteria-Laden Water Interfaces, Physical review Letters, 121, 204502, 2018.

Safi, K. A., Brian Griffiths, F., and Hall, J. A.: Microzooplankton composition, biomass and grazing rates along
495   the WOCE SR3 line between Tasmania and Antarctica, Deep Sea Research Part I: Oceanographic Research Papers, 54, 1025-1041, 10.1016/j.dsr.2007.05.003, 2007.

Salter, Matthew E et al. (2014). "On the seawater temperature dependence of the sea spray aerosol generated by a continuous plunging jet". In : Journal of Geophysical Research : Atmospheres 119.14, p. 9052-9072.

Schulz, M., et al. (2006), Radiative forcing by aerosols as derived from the AeroCom present-day and pre-industrial
500   simulations, Atmos. Chem. Phys., 6, 5225–5246.

Schwier A.N. , K. Sellegri,, S. Mas, B. Charrière, J. Pey, C. Rose, B. Temime-Roussel, D. Parin, J.-L. Jaffrezo, D. Picard, R. Sempéré, N. Marchand and B. D'Anna, "Primary marine aerosol physical and chemical emissions during a nutriment enrichment experiment in mesocosms of the Mediterranean Sea, Atmos. Chem. Phys., 17, 14645-14660, https://doi.org/10.5194/acp-17-14645-2017, 2017

505   Sellegri, K et al. (2006). "Surfactants and submicron sea spray generation". In : Journal of Geophysical Research : Atmospheres 111.D22.

Sellegri, Karine et al. (2021). "Surface ocean microbiota determine cloud precursors". In : Scientific reports 11.1, p. 1-11.

Six, C., Ratin, M., Marie, D., & Corre, E. (2021). Marine Synechococcus picocyanobacteria: Light utilization
510   across latitudes. Proceedings of the National Academy of Sciences of the United States of America, 118(38), 1–
11. https://doi.org/10.1073/pnas.2111300118

Sverdrup, HU (1953). "On conditions for the vernal blooming of phytoplankton". In : J. Cons. Int. Explor. Mer
18.3, p. 287-295.

Thorpe, S. A., Bowyer, P., and Woolf, D. K.: Some factors affecting the size distributions of oceanic bubbles, J.
515   Phys. Oceanogr., 22, 382–389, doi:10.1175/1520- 0485(1992)022<0382:SFATSD>2.0.CO;2, 1992. 16105

Trueblood, Jonathan V et al. (2021). "A two-component parameterization of marine ice-nucleating particles based
on seawater biology and sea spray aerosol measurements in the Mediterranean Sea". In : Atmospheric Chemistry
and Physics 21.6, p. 4659- 4676.

Tyree, Corey A et al. (2007). "Foam droplets generated from natural and artificial seawaters". In : Journal of
520   Geophysical Research : Atmospheres 112.D12.

Wurl, O., Wurl, E., Miller, L., Johnson, K., & Vagle, S. (2011). Formation and global distribution of sea-surface
microlayers. Biogeosciences, 8(1), 121–135. https://doi.org/10.5194/bg-8-121-2011

Yoon, YJ et al. (2006). "Statistical characteristics and predictability of particle formation events at Mace Head". In
: Journal of Geophysical Research : Atmospheres 111.D13.

525   Zábori, Julia, Radovan Krejci et al. (2012). "Wintertime Arctic Ocean sea water properties and primary marine
aerosol concentrations". In : Atmospheric Chemistry and Physics 12.21, p. 10405-10421.

Zábori, Julia, M Matisāns et al. (2012). "Artificial primary marine aerosol production : a laboratory study with
varying water temperature, salinity, and succinic acid concentration". In : Atmospheric Chemistry and Physics
12.22, p. 10709-10724.

530   Zhang, J., Liu, J., Liu, D., Chen, X., Shi, Q., He, C. and Li, G., 2022. Temperature Rise Increases the Bioavailability
of Marine Synechococcus-Derived Dissolved Organic Matter. Frontiers in microbiology, 13.

Zheng, Q., Lin, W., Wang, Y., Li, Y., He, C., Shen, Y., Guo, W., Shi, Q., & Jiao, N. (2021). Highly enriched N-
containing organic molecules of Synechococcus lysates and their rapid transformation by heterotrophic bacteria.
Limnology and Oceanography, 66(2), 335–348. https://doi.org/10.1002/lno.11608

535   Žutić, V., Ćosović, B., Marčenko, E., Bihari, N. and Kršinić, F., 1981. Surfactant production by marine
phytoplankton. Marine Chemistry, 10(6), pp.505-520.

Zwirglmaier, K., Jardillier, L., Ostrowski, M., Mazard, S., Garczarek, L., Vaulot, D., Not, F., Massana, R., Ulloa, O., & Scanlan, D. J. (2008). Global phylogeography of marine Synechococcus and Prochlorococcus reveals a distinct partitioning of lineages among oceanic biomes. Environmental Microbiology, 10(1), 147–161.
540   https://doi.org/https://doi.org/10.1111/j.1462-2920.2007.01440.x

Mode	7-9 °C			2-3°C		
	Dp (nm)	N	σ	Dp	N	σ
Nucleation	10	0,006	1,5	8	0,012	1,5
Aitken	38	0,013	1,6	32	0,019	1,7
Acc1	117	0,027	1,6	108	0,027	1,7
Acc2	290	0,013	1,5	275	0,0115	1,5
Coarse1	1000	0,0095	1,4	850	0,0065	1,4
Coarse 2	2150	0,006	1,4	1800	0,003	1,4

545 **Table 1: Geometric mean diameter (Dp), normalized number concentration (N) and standard deviation (σ) of the 6 modes composing the median number size distribution at moderate (7-9°C) and low (2-3°C) SST.**

550

Atmospheric
Chemistry
and Physics
Discussions
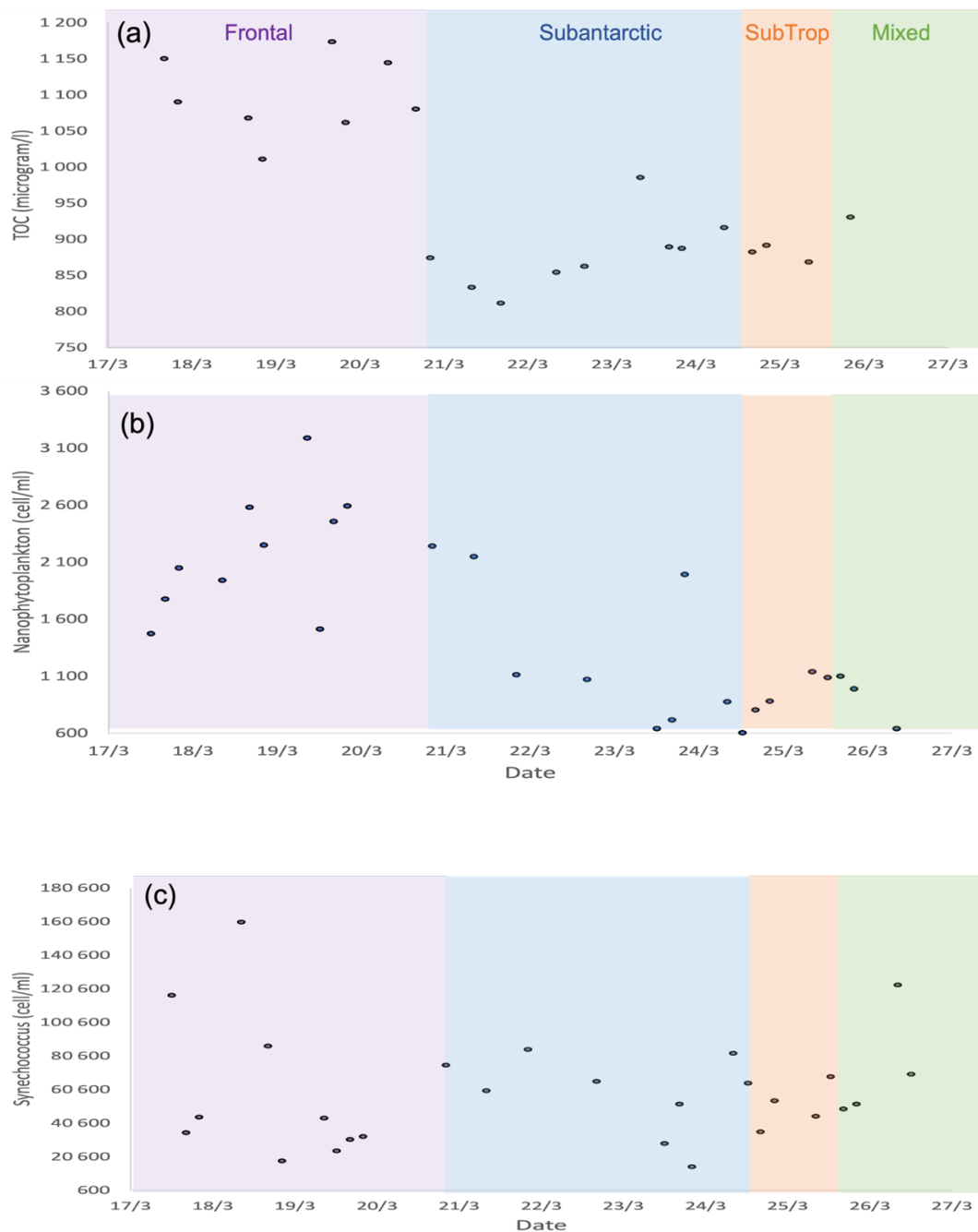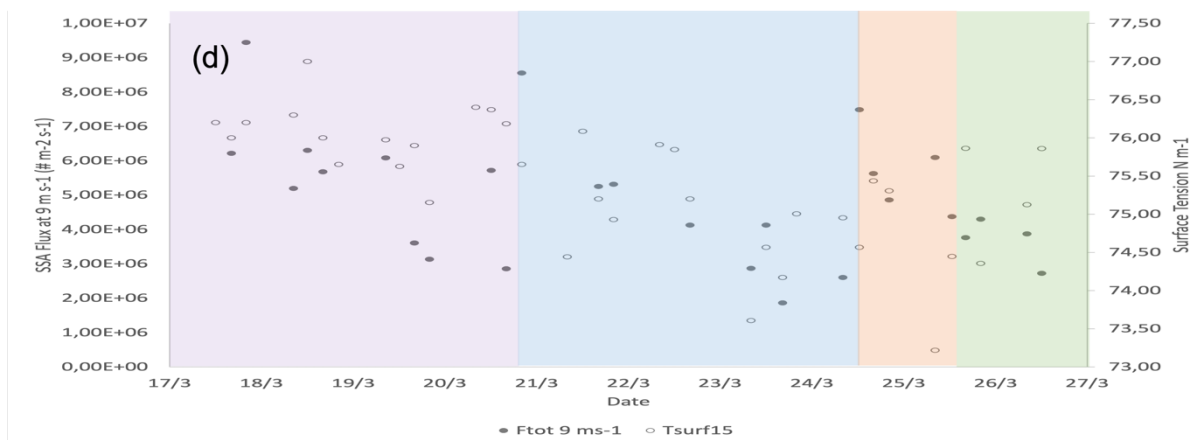
Figure 1: Time series of the seawater (a) TOC content, (b) nanophytoplankton (c) Synechococcus cell abundances and (d) surface tension of seawater samples for SST of 15 °C (right axis), and the SSA flux measured at ambient STT (ranging 13-15°C) and normalized for 9 m s-1 (left axis). Colour-shaded areas represent the different water masses, as indicated by the labels in (a), sampled during the Sea2Cloud voyage (Sellegri et al. 2022).

555
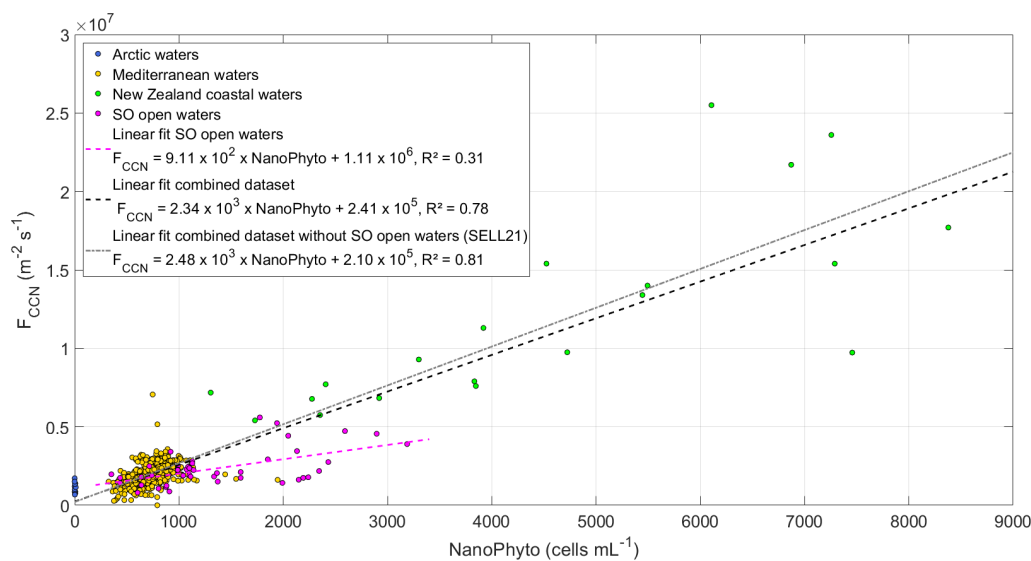
560

Figure 2: SSA-derived CCN number fluxes as a function of NanoPhyto (Nanophytoplankton cell abundance) for the four regional datasets, normalized to an equivalent wind speed of 9 m s⁻¹ and SST of 15°C. The linear fit to the Sea2Cloud data and combined dataset are shown with their corresponding equations and R², with the previously reported SELL21 relationship shown for comparison.
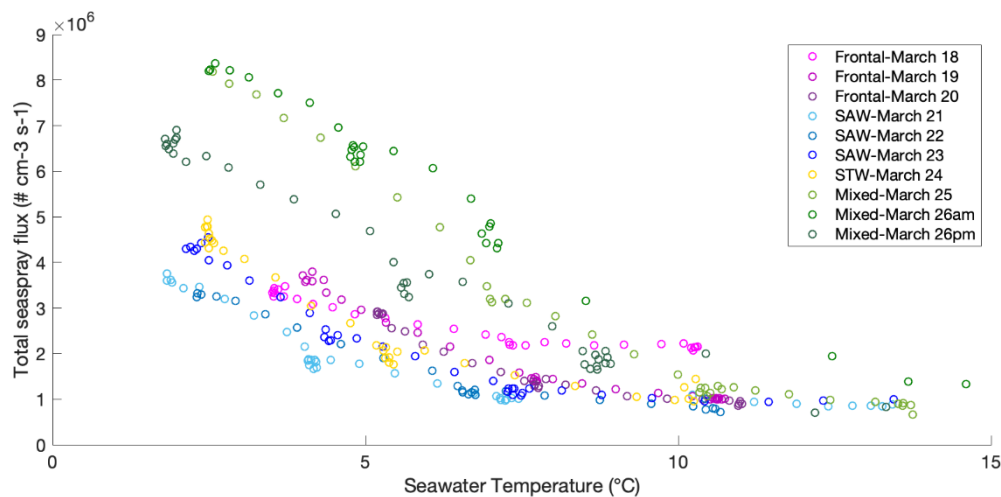
565

Figure 3: Sea-spray number flux as a function of seawater temperature during experiments performed in different water types. Colour code corresponds to water type and dates of sampling as in Figure 1.
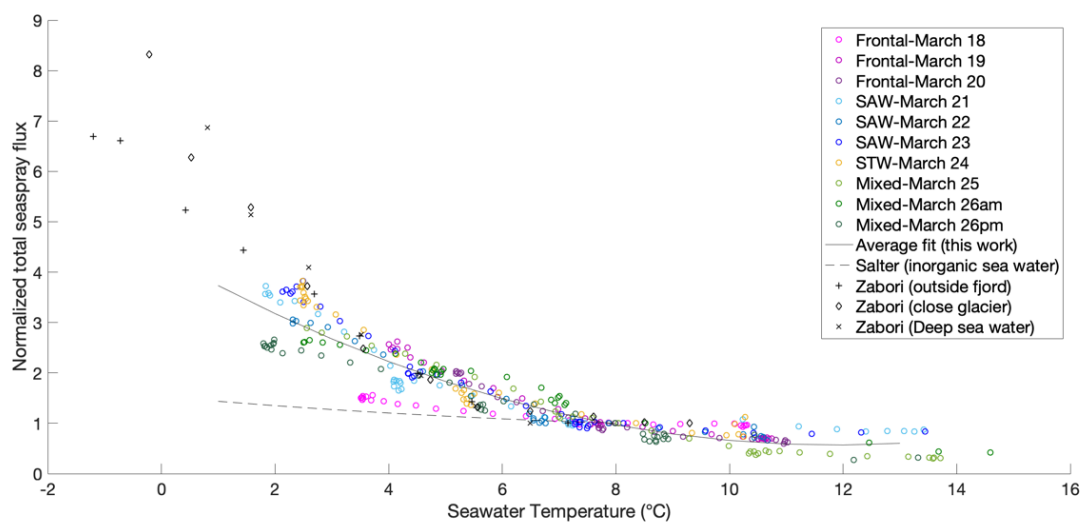
570

23
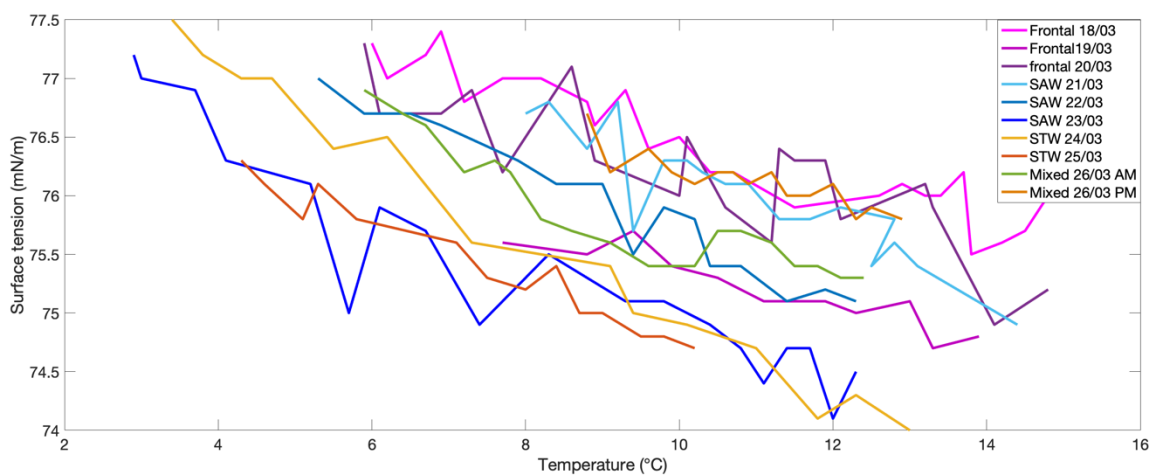
Figure 4: Surface tension in surface seawater at 12:00 LT each day as a function of temperature for different water types.


575

Figure 5: (a) Sea-spray number flux normalized to sea-spray flux measured at 8°C (F_T/F_8) as a function of seawater temperature at different dates and comparison to normalized fluxes (F_T/F_8) reported in Salter et al. (2014) for inorganic seawater and Zabori et al. (2012) for natural arctic seawaters.
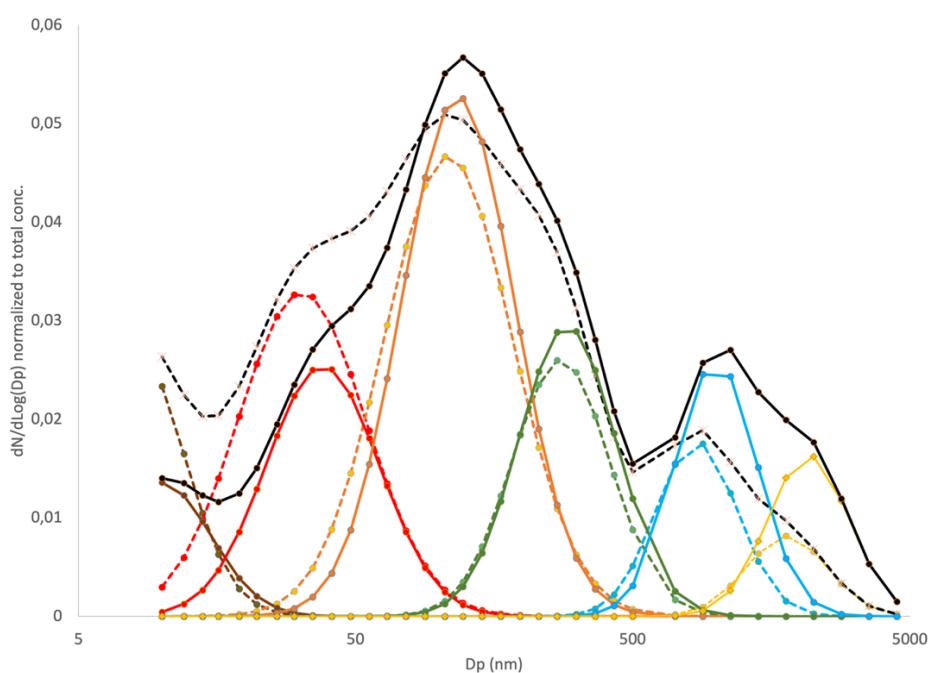
580

Figure 6: Sea-spray size distributions from merged SMPS and WIBS data, normalized to the total sea-spray concentrations and averaged for the temperature range 7 - 9 °C (plain lines) and 2-3 °C (dash lines). Average size distributions were decomposed into single size modes.
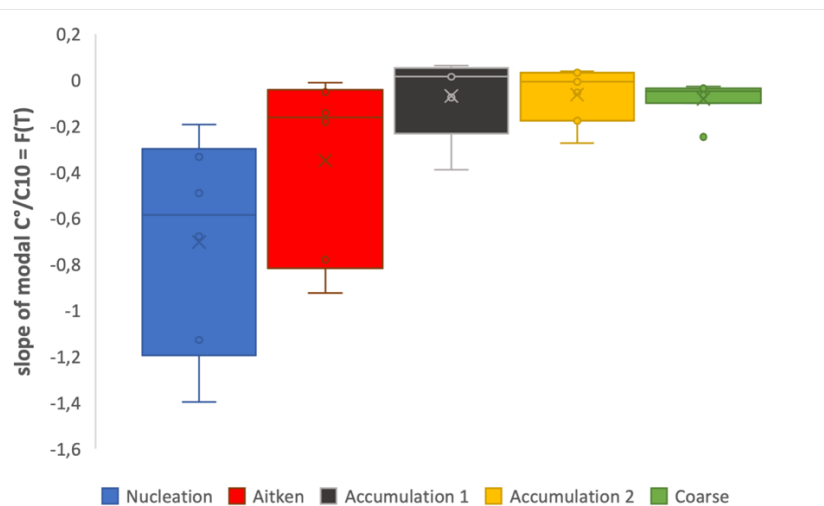
585

Figure 7: Statistics on the slope of modal sea-spray concentrations normalized to modal concentration at 8-10°C.

25